# Dynamics of excited tetrakis(dimethyl amino)ethylene solvated by argon atoms

S. Sorgues, J.-M. Mestdagh, B. Soep, J. P. Visticot

# Dynamics of excited tetrakis(dimethyl amino)ethylene solvated by argon atoms

S. Sorgues, J.-M. Mestdagh, B. Soep, and J.-P. Visticot

*Laboratoire Francis Perrin (CNRS-URA-2453),*
*DSM/DRECAM/Service des Photons, Atomes et Molécules,*
*C.E.A. Saclay,*
*F-91191 Gif-sur-Yvette cedex, France*

**Abstract**

The supersonic expansion of a mixture of the title molecule (TDMAE) with argon generates a beam carrying a log-normal distribution of TDAME$(Ar)_n$ clusters, broadly centered at $\bar{n} \approx 60$. The femtosecond pump-probe technique is used to investigate the excited state dynamics of these clusters up to a 220 ps delay between the pump and the probe. This documents the effect of the argon environment on the TDMAE dynamics. The TDMAE molecule is excited in the valence state V within the cluster by the pump laser at 266 nm. It undergoes deformation in the excited potential energy surface that brings the initial wavepacket to a conical intersection (CI) where the electronic configuration of the molecule switches to a Zwitterionic configuration Z. Compared to the behaviour of free TDMAE, the effect of the argon environment is a slow down of the wavepacket movement and an increase of the time scale of the V-Z energy transfer from 300 fs to $400 \pm 50$ fs. This slow down effect, that we call a *chistera* effect, differs from a standard cage effect. Here, the deforming molecule does not experience a hard sphere collision with the argon cage, rather it pushes it away. Furthermore, umbrella oscillations of the dimethylamino groups are excited when the initial wavepacket passes the CI region. Because of the argon environment, the sharp 250 fs oscillation period of the free molecules is transformed into a broad structure of 40 fs width (FWHM) centred at about 240 fs. In addition, breathing oscillations of the argon environment with respect to the TDMAE molecule are observed with a period of $410 \pm 40$ fs. Finally, long delays between the pump and the probe lasers allow us to investigate the non radiative energy transfer from the Z electronic configuration of TDMAE$(Ar)_n$ to a charge transfer state. The effect of the evaporation of argon atoms in the neutral and the ionised clusters has been taken into account, as its time scale accompanies that of the observed phenomena.

Submitted to Chem. Phys.
Version date: February 26, 2004

# 1 Introduction

Conical intersections (CI) between potential energy surfaces are recognized as playing an ubiquitous and central role in the ultrafast dynamics of electronically excited organic molecules [1–4]. In consequence, ultrafast dynamics can be rationalized as the movement of a vibrational wavepacket along, at least, two deformation coordinates that allows the wavepacket to switch from one potential surface to another. The movement takes place on potential energy surfaces of dimension n, and the switch from one surface to the other is localized in very small regions surrounding CI's of dimension n-2 where two surfaces are exactly degenerate. Such intersections have the dimension n-2, instead of n-1 in standard surface crossings.

Movements, where wavepackets are passing through or near CI's, are routinely invoked on the theoretical side to account for many classes of physical, chemical and biological processes, such as relaxation of electronic energy within molecules [5, 6], steering of photochemical reactions (*e.g.* photoisomerization [7–10] or pericyclic reactions [11]) or light harvesting and energy conversion functions of chromophores in proteins [12, 13]. Controlling the passage of a wavepacket through CI's has even been proposed as a strategy for the optimal control of chemical reactions [14].

In contrast, direct experimental evidence for the passage of vibrational wavepackets through or near CI's is less abundant. It mostly concerns gas phase, femtosecond pump-probe investigations in organic molecules documenting ultrafast energy relaxation processes [15–21], isomerisation reactions [22–25] and ring opening reactions [26–31]. Ethylene [18, 32], substituted ethylene compounds [18–21] and polyenes [22] received a particular attention. One of the most surprising observations is that such wavepacket movements may create observable molecular oscillations when passing either through [33] or near a CI [20].

Although it is not fully documented experimentally, the CI concept is routinely invoked in rather complex situations where the molecule or the molecular group that lead to the CI are embedded in a surrounding medium, a solvent [17,34] or a protein [12,

13]. It may be conceived that the passage of the wavepacket at the CI is affected by the presence of the surrounding medium. Hence, it seems of fundamental importance to examine the reality and the importance of such modifications at a molecular level. Two effects of the solvent are expected. The first one is a direct perturbation of the molecular deformations by the solvent, due to inertial effects. The second one is potentially more profound since it may change the location of CI's that connects surfaces of very different electronic configuration. Charge transfer configurations are likely more stabilised by solvents than other configurations. If a CI connects two such different electronic configurations, this may directly affect the position and shape of the CI, hence influencing the wavepacket movements in the CI region. The present paper aims to examine such effects experimentally and addresses them separately. For this purpose, a model molecule (TDMAE, see below) has been embedded in a model solvent (an argon cluster).

We report here a femtosecond pump/probe investigation where tetrakis(dimethylamino)ethylene molecule (named TDMAE hereafter) is embedded in a significantly large argon cluster (several tens of argon atoms). This work concentrates on the dynamics at conical intersections and relates to the wider research field of solvation effects in ultrafast reaction dynamics [35].

TDMAE is a fairly large polyatomic molecule of structural formula

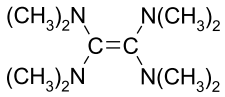


(1)

It is well suited for the present purpose since its ultrafast excited state dynamics is simply an energy relaxation process with no complication due to competing photochemical reaction processes. From earlier experimental work in the present laboratory we know that the 266 nm excitation of TDMAE initiates a wavepacket movement that proceeds on a single potential energy surface with passage near a single CI. There, the electronic configuration switches dramatically from valence to zwitterionic [19]. The time constant of this evolution is 300 fs. Importantly, the wavepacket passage within the CI region is easily probed at either 800 or 400 nm. In the present context, this will allow

us to sensitively investigate how this passage is influenced by the argon environment. Moreover our former experiment on free TDMAE has shown that the deformations that bring the wavepacket near the CI also excite coherently the umbrella oscillation of the dimethylamino groups in TDMAE [20]. Of course observing perturbations to these oscillations when TDMAE is embedded into argon should be another source of information on solvation effects.

The present experiment is run in the gas phase using TDMAE$(Ar)_n$ clusters as the chromophore-solvent model. The cluster technique was used here since it offers the convenient possibility of probing the wavepacket movement by ionisation of TDMAE within the cluster. The counterpart is that the full pump-probe process puts enough energy into the system to stimulate the evaporation of argon atoms. Hence, argon losses will appear as a side effect in the present work and its dynamics must be taken into account for a full interpretation of the present data. In short, the observed ion species result are evaporated ionic species and we have to infer the average size of the initial neutral excited cluster which we investigate.

# 2 Experimental

The experimental apparatus associates a pulsed supersonic beam of TDMAE seeded in argon with a Time-Of-Flight Mass-Spectrometer (TOF-MS). It is coupled to the LUCA femtosecond laser facility of Saclay to perform femtosecond pump-probe experiments.

## 2.1 Laser arrangement

The LUCA laser facility is built around a Titanium-Sapphire regenerative amplifier operating at 800 nm, with a 20 Hz repetition rate. Harmonics at 400 and 266 nm have been generated allowing us for various pump/probe schemes. Two wavelength combinations were used here: 266/800 nm, and 266/400 nm, 266 nm being the pump wavelength. The idea of switching the probe wavelength from 800 to 400 nm was to widen the observation window and to observe coherent molecular oscillations as done

in Ref. [20]. The cross correlation widths of the laser pulses are respectively 120 fs and 140 fs for the 266/800 nm and 266/400 nm wavelength combinations.

The pump and probe laser beams are approximately collinear. They are slightly focused in the extraction zone of the TOF-MS where they cross the molecular beam perpendicularly. The pump laser at 266 nm performs a one photon excitation of the TDMAE molecule within the TDMAE$(Ar)_n$ clusters. The probe laser achieve ionisation to $TDMAE^+$. The power density of the probe at 800 nm is lower than $2 \times 10^{11}$ W cm$^{-2}$, enough to achieve both one- and two-photon ionisation of the electronically excited TDMAE. The much lower power density when probing at 400 nm allows for a one-photon ionisation only.

Finally, a delay line allows us to vary the time delay between the pump and the probe pulses. Positive delays correspond to the probe pulse coming after the pump pulse.

## 2.2 Generation of the TDMAE$(Ar)_n$ clusters

The supersonic beam source enables the co-expansion of a mixture of TDMAE in argon. The gas mixture is performed in the fore-line of the molecular beam. Commercial TDMAE from Aldrich is employed with no further purification, but after thorough outgassing. The beam is operated with an argon backing pressure of 3 bar. The expansion proceeds through a 0.3 mm nozzle, with an opening time of the pulsed valve of 160 $\mu$s. The TOF-MS that allows us to record mass selected ion signals is perpendicular to the molecular beam.

A typical mass spectrum is shown in Figure (1). It has been integrated for pump (266 nm)-probe(800 nm) delays between -200 and +2500 fs. The main peak at 200 amu corresponds to the $TDMAE^+$ ion. It is followed by a series of peaks of general mass $200 + n \times 40$ amu that are attributed to the $TDMAE^+(Ar)_n$ cluster ions. Other peaks are visible also. The peak at 218 amu is due to water impurities and corresponds to $TDMAE^+(H_2O)$. The two large peaks at 288 and 316 amu result from ion-molecule reactions within the $(TDMAE)_2^+$ dimer ion [21], indicating that the neutral $(TDMAE)_2$

dimer is also present in the beam. Hence, the peak at mass 400 amu is not purely due to $TDMAE^+(Ar)_5$ ions ($200 + 5 \times 40$ amu), but contains a contribution from the $(TDMAE)_2^+$ dimer ion ($2 \times 200$ amu) and is not considered further in the present paper. Moreover, under the present pressure conditions, the fraction of TDMAE molecule that appears as TDMAE dimers is believed to be less the 10% of the total number of $TDMAE(Ar)_n$ clusters. We have chosen these conditions because it minimizes the $\frac{TDMAE_n}{TDMAE(Ar]_n}$ ratio.

The series of peaks of general formula, $TDMAE^+(Ar)_n$, observed in Figure (1) has a vanishing intensity near n=13. This does not mean that neutral clusters up to $TDMAE^+(Ar)_{13}$ are only present in the beam. Instead, the neutral cluster distribution may extend to much larger values of n because of two phenomena: *i)* cluster ions can evaporate several argon atoms in the ionisation chamber of the TOF-MS and are therefore detected at smaller masses. *ii)* The detection efficiency of the TOF-MS decreases as the value of n increases because of its perpendicular alignment with respect to the molecular beam.

Assuming that the cluster distribution is not dramatically changed by the presence of TDMAE molecules attached to the clusters, an estimate of the average cluster size $\bar{n}$ can be inferred from empirical formulas treating of the expansion of pure rare gases. Hagena has proposed a dimensionless scaling factor that takes the value $\Gamma^* \approx 1300$ under the present experimental conditions [36]. Using the empirical formula proposed by Buck and Krohne [37], this value leads to the estimate $\bar{n} \approx 60$. This value is consistent with the expectation that the mass spectrum in Figure (1) underestimates the average cluster size. Nevertheless the actual value of $\bar{n}$ could differ from 60, because the presence of TDMAE has certainly biased the cluster distribution and because the expansion is pulsed, whereas the above empirical formula assumes that it is continuous. Nevertheless, the important point here is that a cluster generated from the 3 bar expansion can carry several tens of argon atoms. Moreover, the size distribution of these clusters is expected to be a standard log-normal [38,39] with a full width at half

maximum about equal to the average size $\bar{n}$. In the present case this corresponds to a distribution peaking at $\bar{n} \approx 60$, with 70% of the clusters broadly distributed in the range $25 \leq n \leq 75$. The large size tail of the distribution extends up to n=150 and accounts for additional an 25% of the clusters.

# 3 Results and data analysis

## 3.1 Excited state evolution of TDMAE$(Ar)_n$ clusters probed at 800 nm

Because of the evaporation phenomena that have been mentioned in the previous section, experiments performed on the cluster distribution present in the beam do not show up at the mass of the neutral parents, but at smaller masses. For this reason, we shall see in the discussion that the signals recorded at masses 200 amu (that of $TDMAE^+$) and $200 + 40 \times n$ amu (with n=1–8) that are reported below do reflect the behaviour of clusters taken from the broad cluster distribution present in the beam.

The signal measured at mass 200 amu (n=0) is shown in Figure (2) as a function of the pump(266 nm) - probe(800 nm) delay, up to a 2 ps delay. Signals corresponding to five ions of mass $200 + 40 \times n$ amu are shown in Figure (3) for the same delay range. Data taken up to a 220 ps delay are shown in Figures (4) and (5) for ions of mass 200 and $200 + 40 \times n$ amu respectively.

The signals shown in Figures (2) and (3) can be understood as a bi-exponential decays convoluted by the cross-correlation function of the lasers. For this reason, they can be analyzed using the sequential 3 level scheme that is used in our former publications (see reference [40] and references therein): a level A, initially populated by the pump pulse, decays at a rate $k_A = \frac{1}{\tau_A}$ into a level B which further decays into C at a rate $k_B = \frac{1}{\tau_B}$. Calling $\sigma_A$ and $\sigma_B$ the efficiencies for the ionisation of levels A and B and assuming that C is not ionised, the experimental data can be simulated with

$$\begin{aligned} S(t<0) &= 0 \\ S(t\geq 0) &= \sigma_A \exp(-\tfrac{t}{\tau_A}) + \sigma_B \tfrac{\tau_B}{\tau_B-\tau_A}\left[\exp(-\tfrac{t}{\tau_B}) - \exp(-\tfrac{t}{\tau_A})\right] \quad . \end{aligned} \tag{2}$$

after convoluting S(t) by the cross-correlation function of the lasers. With the timescale

of the figures, the second exponential appears simply as a plateau and only the time constant $\tau_A$ is documented by these fits. The same value $\tau_A = 400 \pm 50$ fs was obtained, for all curves but the fits differ from one curve to the other by the height of the plateau. The latter is in the ratio 0.22:0.78 with respect to the rapid transient for $TDMAE^+$, 0.25:0.75 for $TDMAE^+(Ar)$ and goes down to 0.03:0.97 for $TDMAE^+(Ar)_7$.

The shape of the signal measured at long delay times and shown in Figure (4) is extremely surprising since it departs totally from the bi-exponential decay and the above 3-level scheme cannot apply anymore. We shall see in the discussion that the complexity of this shape is due to evaporation phenomena in the neutral cluster with a time constant in the order of 100 ps. Less spectacular but nevertheless surprising is the shape of the slow tails observed in Figure (5). They appear as an exponential decay with a time constant that depends on which cluster is considered. The relative importance of the slow tail with respect to the rapid first exponential decay, decreases enormously as the cluster size increases. This simply reflects the behaviour observed in the small timescale experiment (see Figure (3)): the height of the plateau decreases as the cluster size increases. For reasons that will appear in the discussion, no attempt is done here to fit the experimental data of the long timescale experiment.

## 3.2 Probing the excited state evolution of $TDMAE(Ar)_n$ at 400 nm

To extend the time window for single photon ionisation, the excited clusters are probed at 400 nm, instead of 800 nm. The top panel in Figure (6) shows the corresponding results when recording signals at mass 200 amu. For comparison the bottom panel of the figure recalls the cluster free results reported in Ref. [20] when argon is replaced by helium. Oscillations are present in both experiments but they are much more distinct in the cluster experiment and their period is different. Figure 7 shows the Fourier transform of the present cluster data after a proper apodisation of the experimental data of Figure (6) to remove the undesired short oscillation periods due both to the rapid raise of the ion signal at short delay, and to the sharp cutoff of the signal at the

longest delay explored experimentally. The main oscillation regime has a 410 fs period. A shoulder on the small value side of the 410 fs peak in the Fourier transform spectrum suggests the existence of a group of unresolved secondary oscillations centred at about 240 fs. The 240 fs period is only twice the cross correlation of the lasers. Hence it is substantially averaged by the apparatus function of the experiment and its apparent weakness in Figure 7 does not reflect its real importance.

Signals have also been recorded with this pump/probe scheme at the mass of $TDMAE^+(Ar)_n$ cluster ions. Unfortunately, the signal-to-noise ratio was quite poor and leads only to the qualitative information that an oscillation regime exists that has apparently the same period than the main oscillation regime of 410 fs observed at mass 200 amu.

# 4 Discussion

The introduction has anticipated that TDMAE acts as a chromophore within the $TDMAE(Ar)_n$ clusters. This is justified by the weakness of the interaction between TDMAE and argon, which is believed to be essentially of van der Waals character. As a corollary to the weakness of the $TDMAE(Ar)_n$ and $TDMAE^+(Ar)_n$ interaction energies, the loss of argon atoms is likely during the pump-probe experiment, either as the cluster is neutral or ionic. This has been mentioned several times already. To be more quantitative on this question, the discussion starts with structure and energetic considerations on the $TDMAE(Ar)_n$ and $TDMAE^+(Ar)_n$ species. Then we discuss the experimental results of the previous section.

## 4.1 Structure and energetics relevant to argon atom losses

### 4.1.1 Structure of the $TDMAE(Ar)_n$ clusters

The question whether the TDMAE molecule is coated by the argon atoms or deposited at the surface of the argon cluster refers to the question of wetting-nonwetting transitions and solvation shell closure in finite systems. To our knowledge this question

has not been addressed for TDMAE in an argon environment, and we are left with comparison with other systems. Such are aromatic molecule-argon systems [41–46]. For example, closure of a first solvent shell about carbazole takes place when n $\approx$ 30 in carbazole$(Ar)_{n=1-36}$ clusters [41]. Nevertheless, open structures corresponding to nonwetting isomers with an incomplete first solvation shell coexist [44, 46]. It is therefore difficult to make a definitive statement upon this question for the TDMAE$(Ar)_n$ clusters from only comparisons with other systems. A semiempirical model based on molecular dynamics calculations was proposed by Perera and Amar to predict the wetting/non wetting character for the solvation of spherical molecules by rare gases [47]. The model compares the Ar-Ar binding energy (12 meV *i.e.* 98 $cm^{-1}$ [48]) and the Ar-Ar equilibrium distance (3.76 Å [48]) to the corresponding quantities in the Arsolute system. The TDMAE-Ar binding energy is estimated as 200 $cm^{-1}$, close to that measured, for example, in the s-tetrazine-Ar van der Waals complex (254 $cm^{-1}$) [49] whereas the TDMAE-Ar equilibrium distance could be estimated as 8 Å(from center to center). With these numbers, the model of Perera and Amar suggests that the TDMAE is embedded in argon. However, the TDMAE is far from spherical and the model does not apply fully. On the other hand, TDMAE should serve as a nucleus for the cluster formation in the seeded argon expansion. We thus consider that TDMAE is substantially if not fully embedded in the argon cluster. In this case, the rearrangement of the clusters during the expansion should favour the formation of a complete first shell about TDMAE rather than a second shell.

With the equilibrium distances given above, 20 to 30 argon atoms should form the first solvation shell and the second shell could carry about 100 additional atoms. Under the present beam conditions, the average cluster size is $\bar{n} \approx 60$ (see section 2.2). Hence, the TDMAE$(Ar_{\bar{n}})$ clusters probably have an essentially completed first shell plus about 40 atoms in the second shell. It is conceivable that the partly completed second solvation shell deviates from a simple layer. Given the broadness of the cluster distribution, the small clusters present in the beam may have a hardly completed first

argon shell whereas the larger may have a half completed second argon shell.

### 4.1.2 Energetics of the $TDMAE(Ar)_n$ and $TDMAE^+(Ar)_n$ clusters

Only $TDMAE(Ar)_n$ clusters of average size n=60 are considered in this section. About 20 argon atoms are expected in the first solvation shell and 40 in the second. A crude estimate of the solvation energy may include only the interaction energies between closest neighbours. The close environment of an argon atom in the first shell could be: the TDMAE molecule, 4 argon atoms of the first shell and 4 argon atoms of the second shell. Considering the binding energies given above, this leads to about 12,000 $cm^{-1}$ of total solvation energy in first solvation shell. With the 40 additional argon atoms of the second shell the total solvation energy becomes 28,000 $cm^{-1}$ ($\approx$ 3.5 eV).

The $TDMAE^+$-Ar binding energy that has not been measured yet, can also be estimated as 450 $cm^{-1}$, *i.e.* close to that found for the aniline$^+$-Ar interaction (520 $cm^{-1}$ [50, 51]). With this value, the total solvation energy of the $TDMAE^+(Ar)_{60}$ cluster ion is 33,000 $cm^{-1}$ $\approx$ 4.1 eV, still assuming that 20 argon atoms are present in the first solvation shell.

With these estimates of the $TDMAE^+(Ar)_{60}$ and $TDMAE(Ar)_{60}$ solvation energies, the adiabatic ionisation potential of $TDMAE(Ar)_{60}$ falls from 5.4 eV for the free TDMAE molecule [52] down to 4.8 eV. The latter value is consistent with the fact that almost no cluster ions are observed with the sole pump laser exciting the cluster beam, an indication that the ionisation energy of the cluster is not significantly smaller than the energy of the 266 nm photons (4.7 eV).

Given the cluster distribution, the adiabatic ionisation energy of the $TDMAE(Ar)_n$ cluster present in the beam is expected to be distributed about 4.8 eV. However, this value in not expected to be any smaller than typically 4.8 eV for the largest clusters present in the beam. Only for the very small clusters, it should differ significantly from 4.8 eV and fall between 4.8 eV and the gas phase value of 5.4 eV. The remaining of the paper deals with pump-probe schemes where the probe ionisation acts on fairly large clusters and proceeds either from a one-photon or a two-photon process. The excess

energy above the ionisation is therefore *ca* 1.4 eV and *ca* 2.9 eV respectively. Some part of it is disposed by the electron and the remainder stays as internal excitation of the cluster ion. This allows for the evaporation of many argon atoms considering that respectively 0.05 eV (400 $cm^{-1}$) and 0.075 eV (600 $cm^{-1}$) are needed to evaporate a second shell and a first shell argon atom. Of course, the two photon probe process is able to induce a substantially more complete evaporation of the cluster ion than the single photon probe.

## 4.2 Solvation effects on the CI passage

Given the assumption that TDMAE acts as a chromophore within the $TDMAE(Ar)_n$ cluster, the picture that serves as a framework for the discussion is the following. The pump laser at 266 nm excites the embedded, or almost embedded TDMAE molecule within a cluster the size of which is broadly distributed about 60 atoms, with about 20 of them in the first solvation shell. The dynamics that follows will be interpreted as a perturbation to the dynamics of free excited TDMAE that is recalled now.

### 4.2.1 A reminder of the free TDMAE dynamics

The femtosecond dynamics of free excited TDMAE has been studied in details in our group [19–21]. The dynamics that takes place during the first few picoseconds following the excitation by the pump laser at 266 nm, has been interpreted within the simple framework of an interplay between electronic configurations of the central CC bond, as that would be the case in regular alkenes. This is justified, given similarities with alkenes. First, structural quantum chemistry studies of similar molecules suggest that TDMAE is quasi planar with respect to the central CC bond. However, the $sp^2$ hybridisation of the central C atoms is constrained, due to the mutual repulsion of the bulky adjacent $CH_3$ groups [53, 54]. Second, the absorption spectrum of TDMAE is dominated by a strong, broad transition peaking near 180 nm [52], close to the $\pi^* \leftarrow \pi$ transition of regular alkenes [55].

Given the above analogy between TDMAE and alkenes, four electronic configura-

tions of the central CC bond are considered: two diradical ones, $\pi\pi^*$ and $(\pi^*)^2$ and two zwitterionic ones, $\Psi_+$ and $\Psi_-$ corresponding to the symmetric and antisymmetric combination of the charge transfer $C^+C^-$ on the central bond. Following the analysis of Salem on the bonding in alkenes, the diradical configurations $\pi\pi^*$ and $(\pi^*)^2$ are dominant respectively in the lowest excited valence singlet state (V) and the doubly excited singlet state (Z) when the 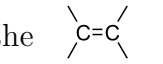 skeleton is planar [56]. Upon torsion, $\pi\pi^*$ and $(\pi^*)^2$ are no longer valid representations of the electronic configuration since the V and Z states receive an increasing contribution of the charge transfer configurations and reach $\Psi_-$ and $\Psi_+$ as dominant character. Both are stabilised by torsion but Z is more stabilised than V, thus resulting into a surface crossing between Z and V along the torsion coordinate. Since the $\Psi_+$ and $\Psi_-$ symmetries are different in this geometry, no coupling occurs between the V and Z states at the crossing. On the other hand, upon pyramidalization of one of the central carbon atoms, the negative charge goes on the pyramidalized carbon, and the $C^+C^-$ versus $C^-C^+$ symmetry is broken. Hence, a coupling appears between the V and Z states. On the basis of two deformation coordinates, torsion about the central CC bond and pyramidalization of one central carbon atoms, the crossing between the V and Z surfaces then appears as a conical intersection (CI).

The interpretation of the dynamics that immediately follows the excitation of TDMAE at 266 nm provided in Ref. [19] follows this picture. Accordingly, the wavepacket that is created by the laser excitation moves on the lower surface of the cone, *i.e.* on a surface that switches from the *V to Z configuration* in the CI region.[1] The time scale of this movement is 300 fs [19]. It has been shown in Ref. [20] that the deformations

[1]Notice a terminology problem arising because a CI is present between the V and Z surfaces. In the Franck-Condon region for excitation from the ground state molecule, V and Z appear as two different excited states of the molecule. However, following the Z surface along the deformation coordinates that define the CI, it is possible to pass the CI and reach the V surface without hopping surfaces. From this point of view, Z and V appear as the same state since they correspond to the same adiabatic surface. For this reason, we prefer to speak of the V and Z configurations and to say that the upper and lower surfaces that define the CI, exchange their character at the CI. Nevertheless, this does not fix the trouble completely since the actual electronic configuration, based on the $\pi\pi^*$, $(\pi^*)^2$, $\Psi_+$ and $\Psi_-$ molecular orbitals changes continuously as the molecule is deformed.

that bring the wavepacket near the CI also excite coherently the umbrella oscillation of the dimethylamino groups. The latter have a 250 fs period, and their damping time, 1.0 ps, is slow compared to the time scale of the V to Z relaxation (300 fs). Rydberg states are also present in this energy region. They may also contribute to the dynamics of excited TDMAE, but their specific role has not been identified yet.

The parallel between TDMAE and alkenes is only approximate since the ionisation energy of TDMAE, 5.4 eV [52], is about 3 eV lower than that of regular alkenes [55]. Likely, such a low ionisation energy is due to delocalisation of the positive charge on the dimethylamino groups of TDMAE whereas the charge is carried by a central C atom in regular alkenes. The possibility of charge delocalisation on the dimethylamino groups also shows up in neutral TDMAE as a charge transfer state CT. In this state, the negative charge is supposed to be carried by a central C atom and the positive charge delocalised on the N atoms. The state CT is below the molecular states built from the V and Z configurations of TDMAE. Its presence likely attracts the descending flux from the Z configuration, hence prevents the Z configuration to decay to the ground state through another CI as extensively documented for regular alkenes [10]. Instead CT is a fluorescent state.

The late dynamics of TDMAE is therefore the following. After the wavepacket has transferred from V to Z, a non radiative decay occurs in 120 ps toward the CT state that fluoresces to ground state at a nanosecond time scale [19].

### 4.2.2 Short time delays: a *chistera* effect on the passage near the CI

The results of the experiment performed in clusters at short pump/probe delays are shown in Figures (2) and (3). The focus is made on the 400 fs time constant transient observed in these figures. The plateau that follows is examined later. *At such short delays between the pump and the probe, argon atoms have not had enough time to evaporate significantly out of the cluster and only argon losses after ionisation will be considered in the present section.*

By comparison to our earlier work on cluster free TDMAE, we anticipate that one

probe photon at 800 nm is sufficient to ionise excited TDMAE within TDMAE$(Ar)_n$ clusters when the molecule has the V configuration, *i.e.* before the wavepacket has reached the CI region where the molecule switches to the Z configuration [19]. This is justified because solvation by argon stabilises ion clusters with respect to the neutral parent, thus lowering the ionisation energy and making the one-photon ionisation in clusters even more likely than in the free molecule. We thus assign the transient in Figures (2) and (3) to the decay from the V to the Z configuration of excited TDMAE within TDMAE$(Ar)_n$ clusters.

The size of the TDMAE$^+(Ar)_n$ ions reported in these figures ranges from n=0 to n=8. It is much smaller than the average size $\overline{n} \approx 60$ of the neutral clusters present in the beam (see section 2.2). Since the cluster distribution in the beam is broad, it could be thought that the TDMAE$(Ar)^+_{1\leq n\leq 8}$ signals reflect the behaviour of very small clusters present in the beam. However, with a single photon ionisation by the probe laser, ions originating from small TDMAE$(Ar)_n$ parents can have an excess energy up to *c.a.* 0.8 eV (0.8 eV is the excess energy for cluster free TDMAE molecule. This excess energy is larger because of the solvation energetics, but 100% of it is not deposited in the cluster ions since the ejected electron takes some energy with). In any case, ions containing such large internal energy cannot survive in the ionisation chamber of the TOF-MS where they spend about 1 $\mu$s, if they have too limited a number of degrees of freedom. Therefore, we believe that Figures (2)-(3) document the dynamics of clusters disposing almost all the available excess energy, that have evaporated many argon atoms in the extraction zone of the TOF-MS. With the energetics provided in section 4.1.2 for large clusters, we infer that the cluster ions appearing at $n \leq 7$ could originate from neutral parent clusters from the small size edge of the distribution that have an almost closed first solvation shell ($\lessapprox$ 20 argon atoms). Larger parents could be considered when adding the thermal energy of the cluster to the available energy for their fragmentation (roughly 0.4 eV when assuming a 30 K temperature). In that case the parent clusters would have several second shell atoms about the closed first

shell.

At this point of the discussion, we are left with the conclusion that the 400 fs transient observed in Figures (2) and (3) reflects the time constant of the V-to-Z relaxation in the environment a closed or an almost closed first solvation shell about the TDMAE molecule. When compared to the 300 fs measured for the same process in the free TDMAE molecule, we thus infer that the argon solvent slows down the relaxation process by 100 fs. This probably results from two antagonistic effects. One is a dielectric effect which stabilizes the Z configuration more efficiently than the V configuration, thus reducing the travel time of the wavepacket towards the CI region. An upper limit, 100 fs, can be given to this effect of stabilization by comparison with our work on the TDMAE dimer where it is at play [21]. The present experimental observations indicate that this effect, if it is significant here, is overwhelmed by a second effect which slows down the wavepacket movement to the CI region. From previous work on the free TDMAE molecule, we know that the excited TDMAE molecule is simultaneously twisting about the CC bond and pyramidalizing about one of the central carbon atoms when it passes by the CI region [19]. To achieve such deformations in the closed shell environment of the molecule, argon atoms have to be moved. Apparently, this slows down the wavepacket movement.

The present effect where the argon atoms that have to be pushed away, are hindering the molecular deformations differ from the usual caging dynamics of a dissociating molecule by a solvent, as exemplified by the dissociation of $I_2$ in rare gases [57, 58] or that of $Cl_2$ molecules within large xenon clusters [59]. The caging dynamics of molecular dissociation appears indeed as a hard sphere collision of the departing halogen atoms with the surrounding atoms. The TDMAE deformations can be slowed down here by the argon environment because of the large size of the dimethyl amino groups that participate to the movement. A parallel can be made with a difference between the tennis game (the usual cage effect) and Basque pelota (the present effect): the tennis ball rebounds on the racket whereas the ball is caught in the wicker basket (the

chistera) of the Basque pelota, slowed down and thrown back.

At a first glance, the *chistera effect* should be unique of clusters, which are free to expand in space. However, a parallel can be made with the mechanism by which an *electronic bubble* develops in response to the excitation of the A(3s$\sigma$) Rydberg orbital of NO within an argon matrix [60]. When considering the early dynamics of the *electronic bubble* in solid argon: *i)* only the first shell responds to the electronic excitation during the first 100 fs following the NO excitation; *ii)* the expansion of the first shell drains 0.33 eV of the available energy; *iii)* the position correlation function of the first shell atoms has a half width of 110 fs. Making an analogy with this situation in the TDMAE$(Ar)_n$ clusters, points *ii)* and *iii)* clearly support that the shell of argon atoms surrounding the TDMAE molecule has a response time in the order of 100 fs which can slow down the V to Z relaxation from 300 fs to 400 fs. Also, the kinetic energy transfered to the expanding argon shell reduces the internal energy of TDMAE after it has switched to the Z configuration.

Photoisomerization of stilbene slowed down by embedment in a cluster or in a solvent was reported in the literature [61–63]. Despite apparent resemblances, the stilbene situation is not fully comparable to the present TDMAE photodynamics. One reason is the complexity of the stilbene photodynamics with a competition exists between the *cis-trans* isomerisation and the isomerisation to dihydrophenantrene. The TDMAE situation is indeed much simpler and should motivate future theoretical calculations: *it involves a wavepacket movement on a single potential surface with a single change of electronic configuration when the wavepacket passes in the vicinity of a CI.*

### 4.2.3 Effect of the *Chistera* catch on the coherent oscillations of the umbrella mode

The dynamics of the TDMAE$(Ar)_n$ clusters is explored now on a wider time window by using the 400 nm probe. This idea was exemplified in our former work on the free TDMAE molecule that revealed an oscillation regime of 250 fs period assigned to the coherent oscillation of the umbrella mode of the dimethylamino groups [20]. We have

interpreted the cluster free experiment as the umbrella motion of the dimethylamino groups, driven into coherent oscillations by two deformations, namely torsion about the central CC bond and pyramidalization about one central carbon atom. These two movements bring the initial wavepacket within the CI region where the system switches from the V to the Z electronic configuration. The two important points in this interpretation are *i)* that the 400 nm photons allow us to probe the TDMAE molecule beyond the surface region where it has transferred to Z and *ii)* that the ionisation cross sections of both the V and Z configurations are sensitive to the umbrella motion of the dimethylamino groups [20]. The latter point is justified by the localisation of the positive charge on the nitrogen atoms of the ground state $TDMAE^+$ ion, which makes the ion less pyramidal about the nitrogen atoms than neutral TDMAE. The excitation of the nitrogen pyramidalization (the umbrella mode) in the neutral molecule thus modulates the Franck-Condon factor for ionisation and therefore modulates the ionisation efficiency, hence enabling the umbrella oscillation to be observed.

The results of the present cluster experiment are shown in Figure (6). The Fourier analysis of its oscillatory behaviour, given in Figure (7), suggests the existence of two oscillation regimes in place of the single 250 fs oscillation observed in the cluster free experiment. One has the period 410 fs and the other corresponds to an unresolved group of oscillations centred at 240 fs. These results are actually expected qualitatively by transposing in the cluster environment the interpretation recalled above for the free TDMAE molecule [20]: the deformations of the TDMAE molecule, torsion and pyramidalization that accompany the V to Z configuration switch near the CI, promotes the coherent umbrella oscillation of the dimethylamino groups, but here, in the presence of an argon environment, the dimethylamino groups that start to vibrate communicate their movement to the surrounding argon atoms, thus exciting a breathing motion of the argon environment with respect to the TDMAE molecule. In turn, the breathing argon environment certainly affects the umbrella motion and the observed oscillatory signals reflect both the umbrella vibration and the environment breathing.

**Data Analysis.** This picture can be modelled very simply as the coupling between two harmonic oscillators. Various choices can be done. All of them end up with the same kind of expression as that below. For example, the coherent umbrella deformations can be described as an elastic oscillator with deformation along an axis $\overrightarrow{x}$, whereas the breathing argon cage environment can be pictured by a second elastic oscillator moving along the axis $\overrightarrow{y}$. The coupling between both oscillators can be simulated by attaching the second oscillator to the moving part of the first one. The coupling strength can be varied by changing the angle between the $\overrightarrow{x}$ and $\overrightarrow{y}$ directions. The general expression describing the movement of the first coupled oscillator is

$$\beta \ \sin^2(\frac{\pi \cdot \mathrm{t}}{\mathrm{T}_{\mathrm{osc}_1}}) + (1-\beta) \ \sin^2(\frac{\pi \cdot \mathrm{t}}{\mathrm{T}_{\mathrm{osc}_2}} + \phi) \tag{3}$$

It oscillates with two periods $\mathrm{T}_{\mathrm{osc}_1}$ and $\mathrm{T}_{\mathrm{osc}_2}$ that are the normal vibrational modes of the coupled oscillators. Of course, these modes are assigned to the periods of 240 and 410 fs measured experimentally. They are deduced from the periods 250 fs and 395 fs of the uncoupled oscillators that are chosen as follows: 250 fs because it is the period of umbrella oscillations of free TDMAE; 395 fs because after coupling with the other oscillator it leads to the 410 fs period measured experimentally. The amplitudes $\beta$ that appear in expression (3) reflect the coupling strength between the oscillators: $\beta = 1$ for the uncoupled oscillators and $\beta = 0.5$ in the case of a strong coupling. $\phi$ is a phase term that reflects the relative position of the oscillators where the umbrella oscillation is excited.

The breathing motion of the argon environment is described by a similar expression to (3). Of course it corresponds to oscillations with the same periods $\mathrm{T}_{\mathrm{osc}_1}$ and $\mathrm{T}_{\mathrm{osc}_2}$ as the umbrella motion, but with different amplitudes and phases. Likely, the breathing motion affects the ionisation cross section of the excited TDMAE molecules, since solvation changes the separation between the molecular and the ionic energy levels. This effect enhances the modulation of the same cross section by the umbrella motion. This does not change the oscillation periods that are observed, but this complicates the

interpretation of their relative amplitude and phase, therefore no attempt was made to unravel this question. On the contrary, the quantities $\beta$ and $\phi$ are considered hereafter as simple fit parameters.

The data of Figure (6) can be analysed by multiplying the detection cross sections $\sigma_{\mathrm{A}}$ and $\sigma_{\mathrm{B}}$ that appear in Expression (2) by the oscillatory factor (3) discussed above. However, the umbrella oscillations are not created by the pump laser excitation, but by the wavepacket descent in its way to the CI region. Hence, the full data analysis must account for an induction time $\tau_{\mathrm{ind}}$ of the oscillations. The data analysis includes also a damping time $\tau_{\mathrm{coh}}$ of the oscillations, and a parameter $\alpha$ that describes the maximum modulation of the cross section that is provoked by the oscillations. The full multiplying factor is therefore:

$$1+\alpha\cdot\left[1-\exp(-\frac{t}{\tau_{ind}})\right]\cdot\exp(-\frac{t}{\tau_{coh}})\cdot\left[\beta\ \sin^2(\frac{\pi\cdot t}{T_{osc1}})+(1-\beta)\ \sin^2(\frac{\pi\cdot t}{T_{osc2}}+\phi)\right] \quad (4)$$

The parameter values that best account for the data in Figure (6) are given in Table (1). The corresponding fits are shown both in Figure (2) (solid line) and on the Fourier analysis of Figure (7) (dashed line). The fair agreement with the experimental results supports the model of coupled oscillators as a tool for the discussion by considering its two main outputs, $\mathrm{T_{osc1}}$ and $\mathrm{T_{osc2}}$.

**A prolongation to the *chistera* effect.** The shortest oscillation period, $\mathrm{T_{osc1}}$, is assigned to the umbrella motion of the TDMAE. Its value $\mathrm{T_{osc1}} = 240$ fs is slightly shorter than the 250 fs oscillation period of the free molecule simply because the coupling between two oscillators makes their eigenfrequencies, hence their oscillation periods more distant than in the uncoupled oscillators. This oscillation regime appears as a fairly broad shoulder in the Fourier analysis shown in Figure (7). This may be the indication that the four dimethylamino groups are not perturbed in exactly the same way by the argon environment.

The longest period, $\mathrm{T_{osc2}}$, is associated with the breathing movement of the argon environment with respect to the TDMAE molecule. The value $\mathrm{T_{osc2}} = 410$ fs can cor-

respond to the excitation of 81 $cm^{-1}$ phonons of the argon environment when assuming that the breathing oscillation regime is harmonic. Several comparisons are done now to clarify the nature of this oscillation.

Firstly the Debye frequency of solid argon is estimated as 64 $cm^{-1}$ after isotopic corrections from a neutron scattering experiment in solid $^{36}Ar$ [64]. It underestimates the present 81 $cm^{-1}$ phonon energy. However, this is not unexpected given that the forces acting on the vibrating shell in $TDMAE(Ar)_n$ are not purely due to the Ar-Ar interaction but also involve the stronger TDMAE-Ar interaction. Moreover, the present experiment does not satisfy the periodic boundary conditions of a macroscopic crystal. For this reason, an useful comparison is the response of solid argon to a localised impulsive deformation that breaks these boundary conditions. Chergui and coworkers have shown indeed that, when the *electronic bubble* develops around an NO impurity in solid argon, the movement of the first argon shell about NO is dominated by a vibration mode of 75 $cm^{-1}$ and the corresponding deformations are mostly radial and very directive [60]. Finally, even closer to the present context, breathing vibrations of argon clusters have been investigated in a collision experiments [65] and both in classical and quantal calculations [66]. Besides high density modes corresponding to the vibration of numerous outer-shell atoms, vibrational modes of smaller density exist that are associated with the inner-shell vibrations of the cluster. In particular, a single mode of 84 $cm^{-1}$ corresponds to the vibration of the central argon atom of the $Ar_{55}$ cluster.

In summary, the TDMAE molecule that starts to deform after the pump pulse plays a similar role with respect to the surrounding argon cluster as the suddenly expanding *electronic bubble* in solid argon: it impulses movement to inner-shell argon atoms and excites the corresponding vibrational modes although their state density is smaller than that of the surface vibrational modes. In fact, the small density of the inner-shell vibrational modes may be a reason why the damping time of the breathing oscillations is fairly slow, 1.5 ps. In passing, this slow damping time is an indication that the argon

environment about the TDMAE molecule is fairly even, as would be a complete first shell. This was a recurrent assumption along this paper.

#### 4.2.4 Long time delays: a probe of solvation effects beyond the passage of the CI in the neutral cluster

The probe wavelength is now back to 800 nm and the pump/probe delay is explored up to 200 ps. The results are shown in Figures (4) and (5). They have two components. *i)* A rapid transient that appears as a single point at the scale of the figures documents on the wavepacket movement before the passage in the CI region, and was discussed in section 4.2.2. *ii)* A slow component follows. It is observed at the $TDMAE^+$ and $TDMAE^+(Ar)_{1-6}$ masses. It appears as a monotonic decay at the cluster ion masses, whereas its behaviour more complex when observed at the $TDMAE^+$ mass.

The slow component observed for the free TDMAE molecule, a simple 120 ps decay, serves as starting point for the discussion of the present slow component. It was assigned to the decay of the Z population, due to an energy transfer toward the CT state [19]. In this interpretation, the low energy Z configuration of TDMAE is ionised by two probe photons at 800 nm. The mechanism responsible for transferring population from Z to CT is likely a non radiative intramolecular conversion that operates at the statistical regime as described by Jortner *et al* [67].

A simple transposition of this interpretation to the present cluster experiment suggests that the slow component observed in Figures (4) and (5) documents the electronic relaxation to CT after the excited $TDMAE(Ar)_n$ system has switched to the Z configuration. Again a 2-photon ionisation is assumed. This provides up to 2.9 eV excess energy in the cluster ion and enables the evaporation of many argon atoms as stated at the end of section 4.1.2. Hence, the present slow component can be understood as the fingerprint of the Z-to-CT energy transfer in the presence of argon atom losses. A simple RRKM calculation suggests that up to 10 or 15 argon atoms can be evaporated during the 200 ps following the pump excitation. Of course, each evaporation of an argon atom cools down the remaining $TDMAE(Ar)_{<n}$ cluster, hence reducing the rate

of the Z-to-CT transfer that damps the Z population. The Z-to-CT transfer, which was assigned to a statistical intramolecular conversion process is likely highly dependent on the excess energy through the Franck Condon overlap of the bath modes in the initial and final states. This might be a reason why the $TDMAE^+$ and $TDMAE^+(Ar)_{1-4}$ signals have not fallen down to zero after 200 ps (see Figures (4) and (5)). Simply, the slowed down Z-to-CT energy transfer has had not enough time in 200 ps to evacuate all the Z population of the evaporating neutral parents. The resulting slow component is complex and difficult to interpret quantitatively, since evaporated clusters of various sizes and internal energies contribute to the signals observed experimentally. Two observations are striking in that sense: *i)* the slow decays of Figure (5) are monotonic but depend on the size of the cluster ions where the observation is done. *ii)* The slow tail in the $TDMAE^+$ signal shown in Figure (4) is not even monotonic.

The latter observation deserves a comment for ending the discussion since it reveals a peculiarity of the probe process. Two probe pathways must be considered in an evaporating cluster experiment when timescales of several hundreds of picoseconds are considered [68]. In the first one, the excited $TDMAE(Ar)_n$ is probed before evaporating argon atoms and the full argon evaporation occurs from the ionised $TDMAE^+(Ar)_n$. In the second pathway, evaporation of a few argon atoms occurs before the ionisation and the remaining argon atoms are lost after the ionisation. The increase of the signal between 10 and 130 ps in Figure (4) could be the indication that the second pathway has a larger cross section than the first one. When the repopulation of excited small neutral clusters by larger clusters is overwhelmed by the overall decay of the Z population, then a signal decay is observed as it is the case when the pump-probe delay is larger than 130 ps.

# 5 Summary and conclusion

The supersonic expansion of a mixture of tetrakis(dimethylamino)ethylene (TDMAE) with argon generates a beam carrying a log-normal distribution of $TDAME(Ar)_n$ clus-

ters, with broadly peaking near $\bar{n} \approx 60$ . The femtosecond pump-probe technique is used to investigate the excited state dynamics of these clusters up to 220 ps delay between the pump and the probe. The aim of the work is to document the effect of a solvent on the dynamics of a vibrational wavepacket that travels close to a conical intersection connecting to potential surfaces. In this study, the argon cluster acts as a model solvent and TDMAE was chosen because its ultrafast excited dynamics as a free molecule is well documented and can be described very simply by a wavepacket movement near a conical intersection (CI).

The TDMAE molecule is excited to the valence state V within the cluster by the pump laser at 266 nm. It undergoes deformation along, at least, two coordinates in the excited surface that brings the initial vibrational wavepacket to the CI where the electronic configuration of the molecule switches to a Zwitterionic configuration Z. Compared to the behaviour of free TDMAE, the effect of the argon environment is to slow down the wavepacket movement and to increase the time scale of the energy transfer from 300 fs to 400 fs. In our opinion, this effect of the argon environment differs from the *cage effect* that is often invoked when dealing with solvent effects. In the present case indeed, the deforming molecule does not seem to experience a true collision with the argon cage and to rebound on it. Instead, it moves the argon atoms as it deforms. We called this a *chistera* effect, in analogy to the basque pelota game, to stress that the argon atoms of the cluster are accompanying the deforming molecule. Still considering analogies, the deforming TDMAE molecule plays a role comparable to that of an expanding *electronic bubble* in solid argon [60].

Our former work on the free TDMAE molecule showed that the wavepacket passage in the CI region coherently excites the umbrella oscillation of the dimethylamino groups. In the present cluster experiment, this oscillator is coupled to other oscillators describing deformations of the argon environment: the 250 fs oscillation period of the free molecules is broadened in the present work and gets a central period of 240 fs; moreover, breathing oscillations of the argon environment with respect to the TDMAE

molecule are observed with a period of 410 fs. The *chistera* picture and the analogy with the *electronic bubble* have helped to provide a likely interpretation to these results. The TDMAE molecule is deforming after the pump excitation and moves the argon atoms that are coating it. This deformation, a twist about the central CC bond and a pyramidalization about one of the central C atoms brings the initial vibrational wavepacket towards a conical intersection, exciting simultaneously an oscillation of the molecule along a third coordinate, the umbrella deformation of the dimethylamino groups. This oscillation moves coherently the entire first shell of argon atoms that starts in turn to oscillate with a 410 fs period and a 1.5 ps coherence time.

Finally, measurements at the long delays between the pump and the probe laser allows us to investigate the non radiative energy transfer from the Z electronic configuration of TDMAE$(Ar)_n$ to a charge transfer state CT. This process also exists in cluster free TDMAE and occurs with a 120 ps time constant through a statistical non radiative process. Again, the effect of the argon environment is to slow down the process and the decay time from Z to CT then exceeds 200 ps. However, unlike the previous *chistera* effect, the origin of the present slow down process could be simply the cooling of the TDMAE molecule due to the evaporation of argon atoms in neutral TDMAE$(Ar)_n$ that occurs at the same time scale as the Z to CT energy transfer.

# Acknowledgments

The authors are happy to thank O. Gobert, P. Meynadier and M. Perdrix, who are responsible for developing, maintaining and running the femtosecond laser facility LUCA (Laser Ultra-Court Accordable) of the CEA, DSM/DRECAM. This work is partly supported by the European Community through the PICNIC network (Product Imaging and Correlation: Non-adiabatic Interactions in Chemistry) under contract number HPRN-CT-2002-00183.

# References


[1] M. Olivucci, F. Bernardi, and M. A. Robb, THEOCHEM **463**, 42 (1999).

[2] S. Zilberg and Y. Haas, Chem. Eur. J. **5**, 1755 (1999).

[3] D. R. Yarkony, J. Phys. Chem. A **105**, 6277 (2001).

[4] B. E. Applegate, T. A. Barckholtz, and T. A. Miller, Chem. Soc. Rev. **32**, 38 (2003).

[5] F. Bernardi, M. Olivucci, and M. A. Robb, Chem. Soc. Rev. **25**, 321 (1996).

[6] M. J. Bearpark, F. Bernardi, S. Clifford, M. Olivucci, M. A. Robb, B. R. Smith, and T. Vreven, J. Am. Chem. Soc. **118**, 169 (1996).

[7] M. J. Bearpark, F. Bernardi, S. Clifford, M. Olivucci, M. A. Robb, and T. Vreven, J. Phys. Chem. A **101**, 3841 (1997).

[8] J. Quenneville, M. Ben-Nun, and T. J. Martínez, J. Photochem. Photobiol. A-Chem. **144**, 229 (2001).

[9] M. Ben-Nun and T. J. Martínez, Ab initio quantum molecular dynamics, in *Advances in Chemical Physics, Volume 121*, volume 121 of *Advances in Chemical Physics*, pages 439–512, JOHN WILEY & SONS INC, New York, 2002.

[10] J. Quenneville and T. J. Martínez, J. Phys. Chem. A **107**, 829 (2003).

[11] F. Bernardi, M. Olivucci, and M. A. Robb, J. Photochem. Photobiol., A **105**, 365 (1997).

[12] K. Winkler, J. R. Lindner, V. Subramaniam, T. M. Jovin, and P. Vohringer, Phys. Chem. Chem. Phys. **4**, 1072 (2002).

[13] T. Polivka, D. Zigmantas, J. L. Herek, Z. He, T. Pascher, T. Pullerits, R. J. Cogdell, H. A. Frank, and V. Sundstrom, J. Phys. Chem. B **106**, 11016 (2002).

[14] Roland Mitrić, Michael Hartmann, and Vlasta Pittner, Jirìand Bonacic-Koutecký, J. Phys. Chem. A **106**, 10477 (2002).

[15] E. W.-G. Diau, S. De Feyter, and A. H. Zewail, J. Chem. Phys. **110**, 9785 (1999).

[16] A. J. Wurzer, T. Wilhelm, J. Piel, and E. Riedle, Chem. Phys. Lett. **299**, 296 (1999).

[17] Hyuk Kang, Boyong Jung, and Seong Keun Kim, J. Chem. Phys. **118**, 6717 (2003).

[18] J. M. Mestdagh, J. P. Visticot, M. Elhanine, and B. Soep, J. Chem. Phys. **113**, 237 (2000).

[19] B. Soep, J. M. Mestdagh, S. Sorgues, and J. P. Visticot, Eur. Phys. J. D **14**, 191 (2001).

[20] S. Sorgues, J. M. Mestdagh, J. P. Visticot, and B. Soep, Phys. Rev. Lett. **91**, 103001 (2003).

[21] S. Sorgues, J. M. Mestdagh, E. Gloaguen, M. Heninger, H. Mestdagh, J. P. Visticot, and B. Soep, Submitted to J. Phys. Chem. A, 2003.

[22] W. Fuss, S. Lochbrunner, A. M. Muller, T. Schikarski, W. E. Schmid, and S. A. Trushin, Chem. Phys. **232**, 161 (1998).

[23] W. Fuss, K. L. Kompa, T. Schikarski, W. E. Schmid, and S. A. Trushin, Proc. SPIE-Int. Soc. Opt. Eng. **3271**, 114 (1998).

[24] W. Fuss, K. L. Kompa, T. Schikarski, W. E. Schmid, and S. A. Trushin, Springer Ser. Chem. Phys. **63**, 615 (1998).

[25] Mirianas Chachisvilis and Ahmed H. Zewail, J. Phys. Chem. A **103**, 7408 (1999).

[26] W. Fuss, T. Schikarski, W. E. Schmid, S. Trushin, and K. L. Kompa, Chem. Phys. Lett. **262**, 675 (1996).

[27] S. A. Trushin, W. Fuss, T. Schikarski, W. E. Schmid, and K. L. Kompa, J. Chem. Phys. **106**, 9386 (1997).

[28] W. Fuss, P. Hering, K. L. Kompa, S. Lochbrunner, T. Schikarski, W. E. Schmid, and Sergei A. Trushin, Ber. Bunsen-Ges. **101**, 500 (1997).

[29] Zhong Dongping, Ew G. Diau, T. M. Bernhardt, S. De Feyter, J. D. Roberts, and A. H. Zewail, Chem. Phys. Lett. **298**, 129 (1998).

[30] D. Zhong, E. W.-G. Diau, T. M. Bernhardt, S. De Feyter, J. D. Roberts, and A. H. Zewail, Chem. Phys. Lett. **298**, 129 (1998).

[31] Ew G. Diau, S. De Feyter, and A. H. Zewail, Chem. Phys. Lett. **304**, 134 (1999).

[32] P. Farmanara, V. Stert, and W. Radloff, Chem. Phys. Lett. **288**, 518 (1998).

[33] S. A. Trushin, T. Yatsuhashi, W. Fuss, and W. E. Schmid, Chem. Phys. Lett. **376**, 282 (2003).

[34] H. Bouas-Laurent, A. Castellan, J. P. Desvergne, and R. Lapouyade, Chem. Soc. Rev. **30**, 248 (2001).

[35] Q. Zhong and A. W. Castleman, Chem. Rev. **100**, 4039 (2000).

[36] O. F. Hagena, Z. Phys. D **4**, 291 (1987).

[37] U. Buck and R. Krohne, J. Chem. Phys. **105**, 5408 (1996).

[38] J. Gspann, , in *Physics of Electronic and Atomic Collisions*, edited by S. Datz, pages 43–45, North-Holland, Amsterdam, 1982.

[39] K. J. Mendham, N. Hay, M. B. Mason, J. W. G. Tisch, and J. P. Marangos, Phys. Rev. A **64**, 055201 (2001).

[40] J. M. Mestdagh, J. P. Visticot, M. Elhanine, and B. Soep, J. Chem. Phys. **113**, 237 (2000).

[41] S. Leutwyler and J. Bosiger, Faraday Discussions of the Chemical Society **86**, 225 (1988).

[42] U. Even, N. Ben-Horin, and J. Jortner, Chem. Phys. Lett. **156**, 128 (1989).

[43] J. E. Adams and R. M. Stratt, J. Chem. Phys. **93**, 1358 (1990).

[44] N. Ben-Horin, U. Even, J. Jortner, and S. Leutwyler, J. Chem. Phys. **97**, 5296 (1992).

[45] C. Guillaume, M. Mons, J. Le-Calve, and I. Dimicoli, J. Phys. Chem. **97**, 5193 (1993).

[46] M. Schmidt, J. Le-Calve, and M. Mons, J. Chem. Phys. **98**, 6102 (1993).

[47] L. Perera and F. G. Amar, J. Chem. Phys. **93**, 4884 (1990).

[48] U. Buck, Elastic scattering, in *Molecular Scattering; Physical and Chemical Applications*, edited by K. P. Lawley, chapter , pages 313–388, Wiley, Chichester,Sussex,England, 1975.

[49] D.V. Brumbaugh, J.E. Kenny, and D.H. Levy, J. Chem. Phys. **78**, 3415 (1983).

[50] S. Douin, P. Parneix, and P. Bréchignac, Z. Phys. D **21**, 343 (1991).

[51] N. Solca and O. Dopfer, Eur. Phys. J. D **20**, 469 (2002).

[52] Y. Nakato, M. Ozaki, and H. Tsubomura, Bull. Chem. Soc. Jap. **45**, 1229 (1972).

[53] H. Bock, H. Borrmann, H. Oberhammer, Z. Havlas, K. Ruppert, and A. Simon, Angew. Chem. Int. ed. Engl. **30**, 1678 (1991).

[54] P. Fleurat-Lessard and F. Volatron, J. Phys. Chem. A **102**, 10151 (1998).

[55] M. B. Robin, *Higher Excited States of Polyatomic Molecules, Vol. 2*, Academic press, New York, USA, 1975.

[56] L. Salem, *Electrons in Chemical Reactions: First Principles*, John Wiley and Sons, New York, 1982.

[57] Q. Liu, J. K. Wang, and A. H. Zewail, Nature **364**, 427 (1993).

[58] R. Zadoyan, Z. Li, C. C. Martens, and V. A. Apkarian, J. Chem. Phys. **101**, 6648 (1994).

[59] J. M. Mestdagh, M. Berdah, C. Dedonder-Lardeux, C. Jouvet, S. Martrenchard-Barra, D. Solgadi, and J. P. Visticot, Eur. Phys. J. D **4**, 291 (1998).

[60] S. Jimenez, M. Chergui, G. Rojas-Lorenzo, and J. Rubayo-Soneira, J. Chem. Phys. **114**, 5264 (2001).

[61] J. K. Rice and A. P. Baronavski, J. Phys. Chem. **96**, 3359 (1992).

[62] D. C. Todd and G. R. Fleming, J. Chem. Phys. **98**, 269 (1993).

[63] A. A. Heikal, S. H. Chong, J. S. Baskin, and A. H. Zewail, Chem. Phys. Lett. **242**, 380 (1995).

[64] Y. Fujii, N. A. Lurie, R. Pynn, and G. Shirane, Phys. Rev. B **10**, 3647 (1974).

[65] Udo Buck, R. Krohne, and P. Lohbrand, J. Chem. Phys. **106**, 3205 (1997).

[66] T. Schröder, R. Schinke, R. Krohne, and Udo Buck, J. Chem. Phys. **106**, 9067 (1997).

[67] J. Jortner, S.A. Rice, and R.M. Hochstrasser, Adv. Photochem. **7**, 149 (1969).

[68] G. Grégoire, M. Mons, I. Dimicoli, C. Dedonder-Lardeux, C. Jouvet, S. Martrenchard, and S. Solgadi, J. Chem. Phys. **110**, 1521 (1999).

# TABLES

| | Free TDMAE | $TDMAE(Ar)_n$ Clusters |
|---|---|---|
| $\tau_A$ | 300 fs | $400 \pm 50$ fs |
| $\tau_B$ | 120 ps | $\gg 10$ ps |
| $\frac{\sigma_A}{\sigma_B}$ | 2.0 | $0.65 \pm 0.2$ |
| $\alpha$ | 0.7 | $1.1 \pm 0.1$ |
| $\tau_{ind}$ | 30 fs | $50 \pm 40$ fs |
| $\tau_{coh}$ | 1 ps | $1.5 \pm 0.2$ ps |
| $T_{osc1}$ | 250 fs | $240 \pm 30$ fs |
| $T_{osc2}$ | | $410 \pm 20$ fs |
| $\beta$ | | $0.35 \pm 0.05$ |
| $\phi$ | | $-\frac{\pi}{6}$ |

Table 1: Best parameters to fit the experimental data of Figure (6) using expressions 2 and 4. See the text for details. The numbers for the free TDMAE experiment are taken from Ref. [20].

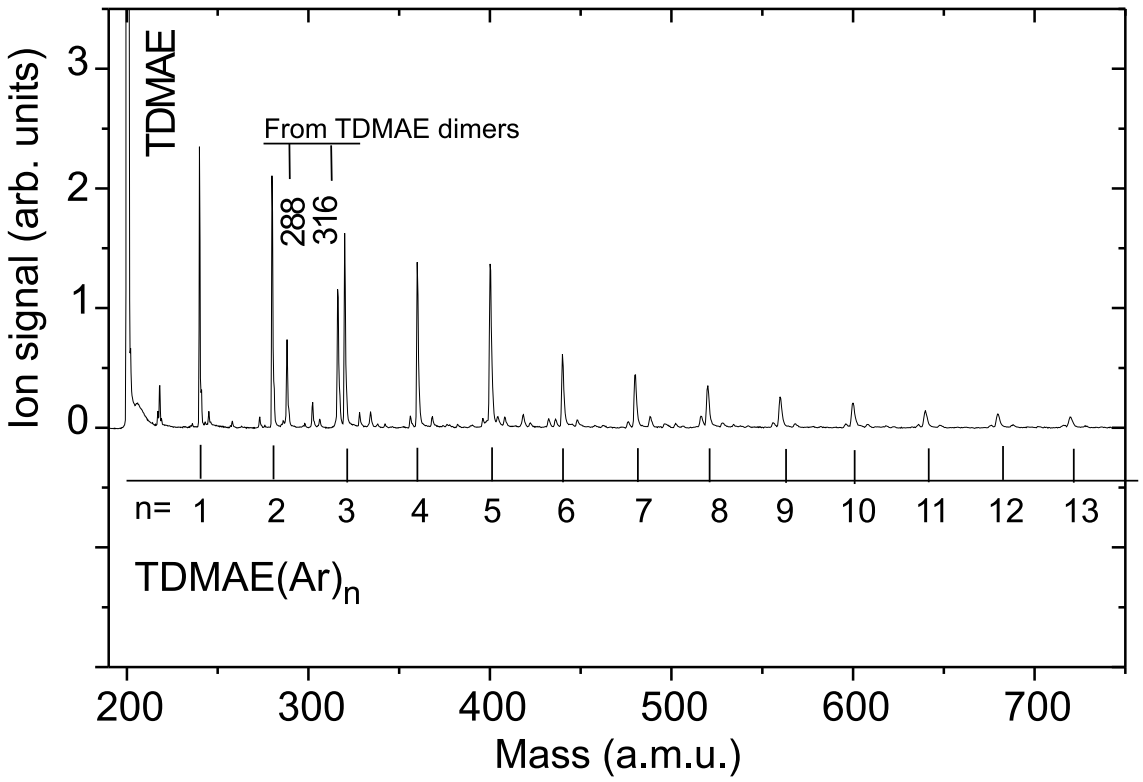


Figure 1: Mass spectrum observed upon ionisation of the TDMAE/argon beam with 266+800 nm femtosecond pulses. The argon backing pressure is 3 bars.

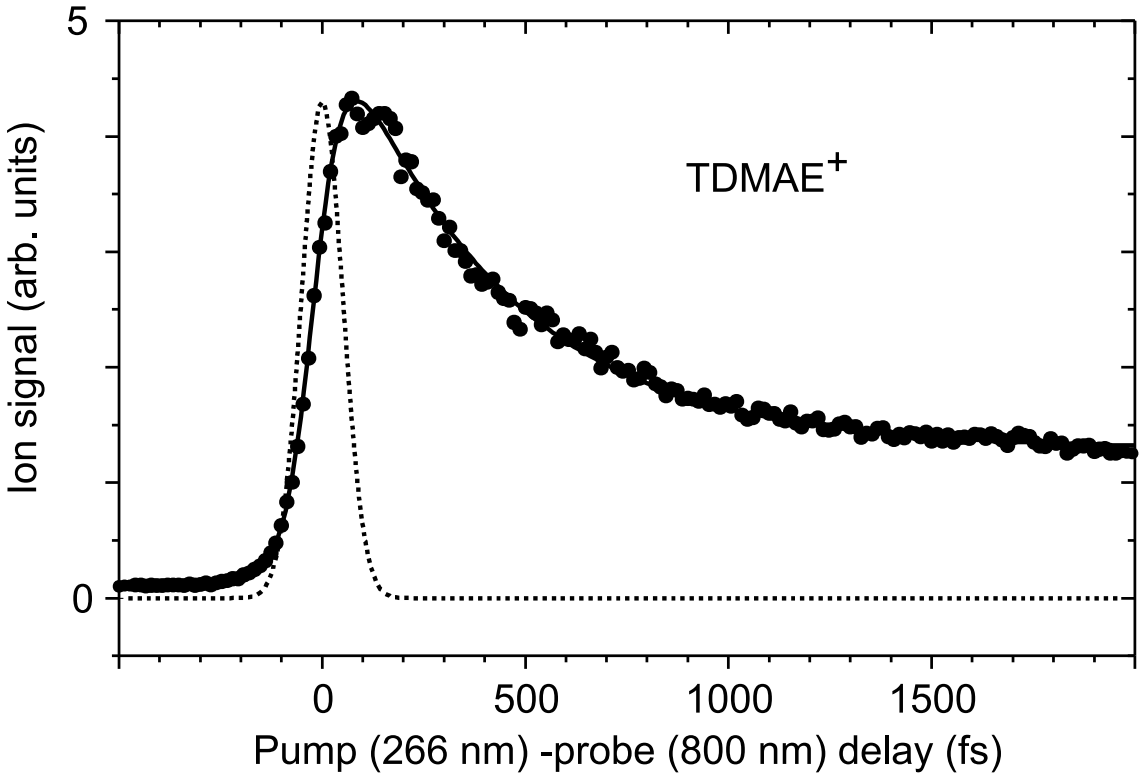


Figure 2: Evolution of the signal measured at the mass of $TDMAE^+$ as a function of the pump (266 nm)-probe (800 nm) delay. The solid line passing through the experimental data is a fit using expression 2 that corresponds to $\tau_A = 400 \pm 50$ fs. The dotted curve shows the cross correlation function of the lasers.

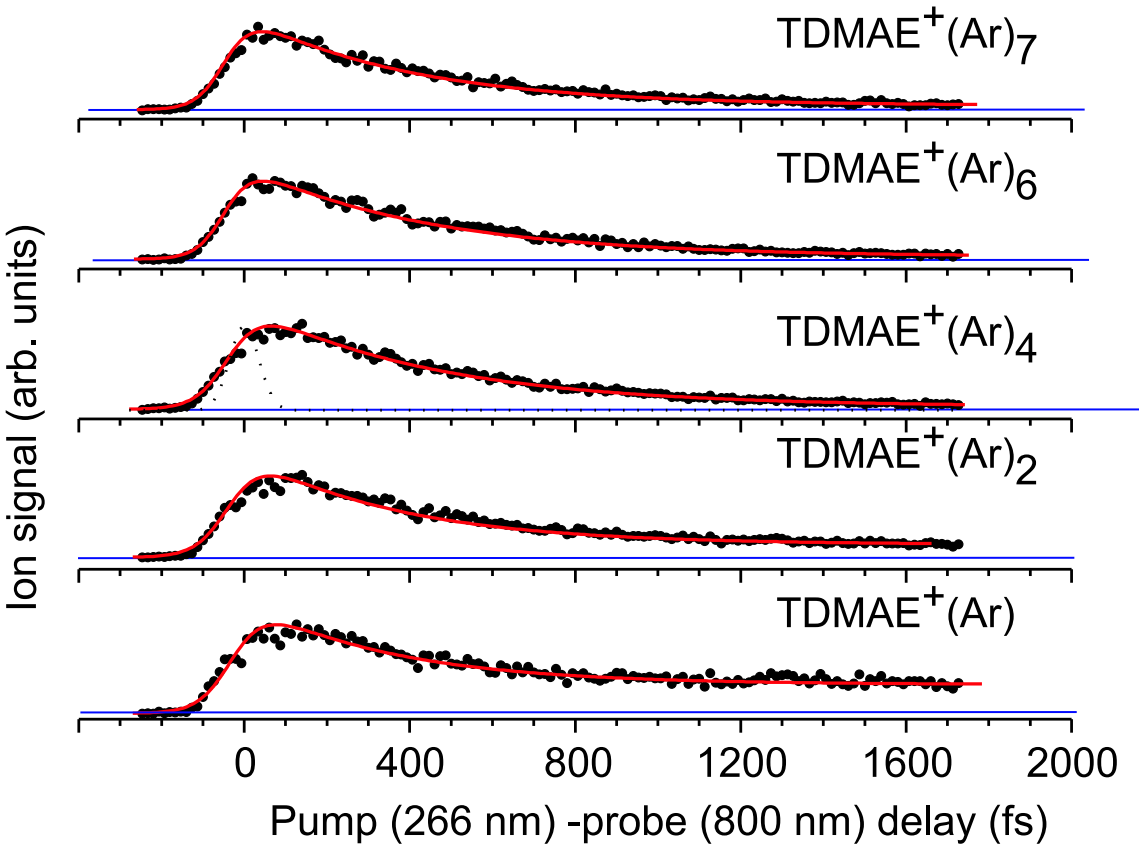


Figure 3: Evolution of the signal measured at the mass of $TDMAE^+(Ar)_n$ as a function of the pump (266 nm)-probe (800 nm) delay. The value of n is labelled in the figure. The solid line running through the experimental data is a fit using using expression 2. Whatever the curve that is concerned, it correspond to $\tau_A = 400 \pm 50$ fs. The dotted curve in the $TDMAE^+(Ar)_4$ figure shows the cross correlation function of the lasers.

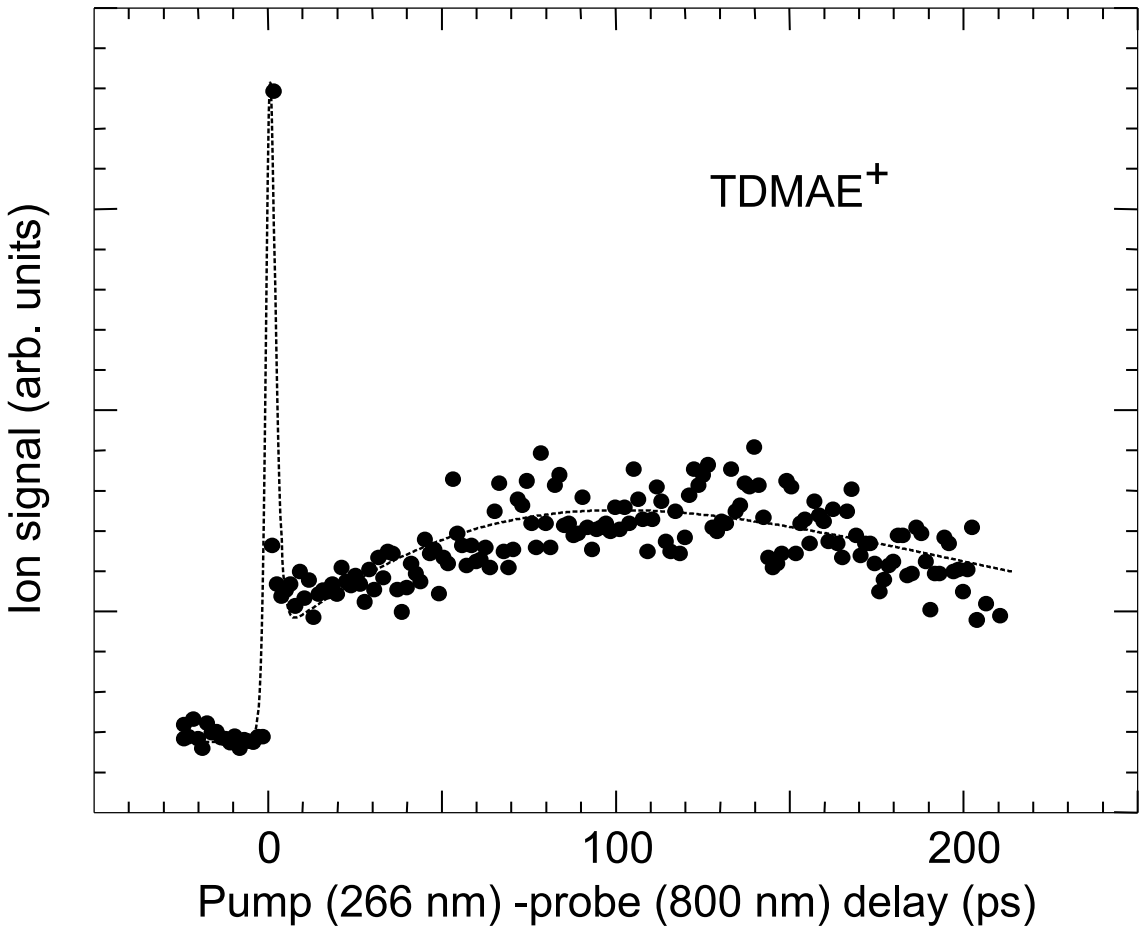


Figure 4: Evolution of the signal measured at the mass of $TDMAE^+$ as a function of the pump (266 nm)-probe (800 nm) delay. The dashed line passing through the experimental data is a fit.

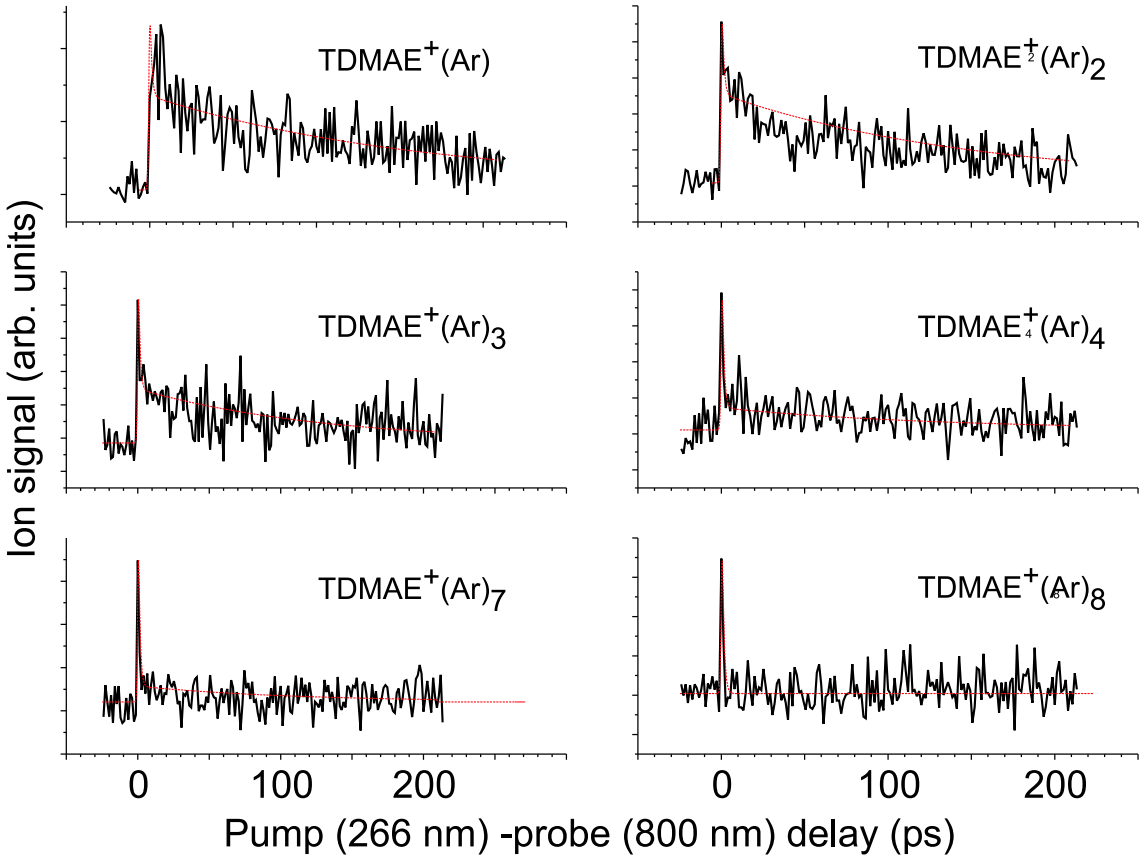


Figure 5: Evolution of the signal measured at the mass of $TDMAE^+(Ar)_n$ as a function of the pump (266 nm)-probe (800 nm) delay. The value of n is labelled in the figures. The dashed line running through the experimental data is a fit.

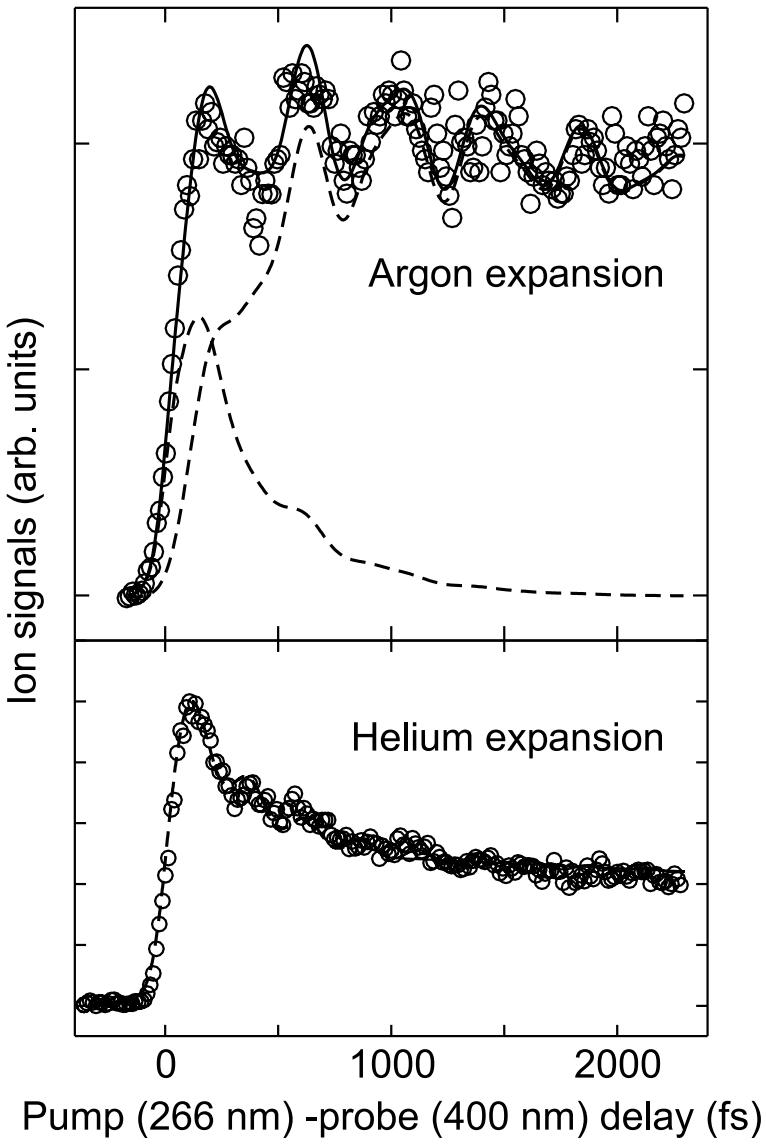


Figure 6: Evolution of the signal measured at the mass of $TDMAE^+$ as a function of the pump (266 nm)-probe (400 nm) delay. The top panel shows the present cluster experiment. The solid line passing through the experimental points is a fit using Expressions (2) and (4) with the parameters listed in Table (1). The dashed curves are the contributions that appear in Expression (2) with the cross sections $\sigma_{\mathrm{A}}$ and $\sigma_{\mathrm{B}}$. The bottom panel recalls cluster free results when the TDMAE beam was generated in a helium expansion [20].

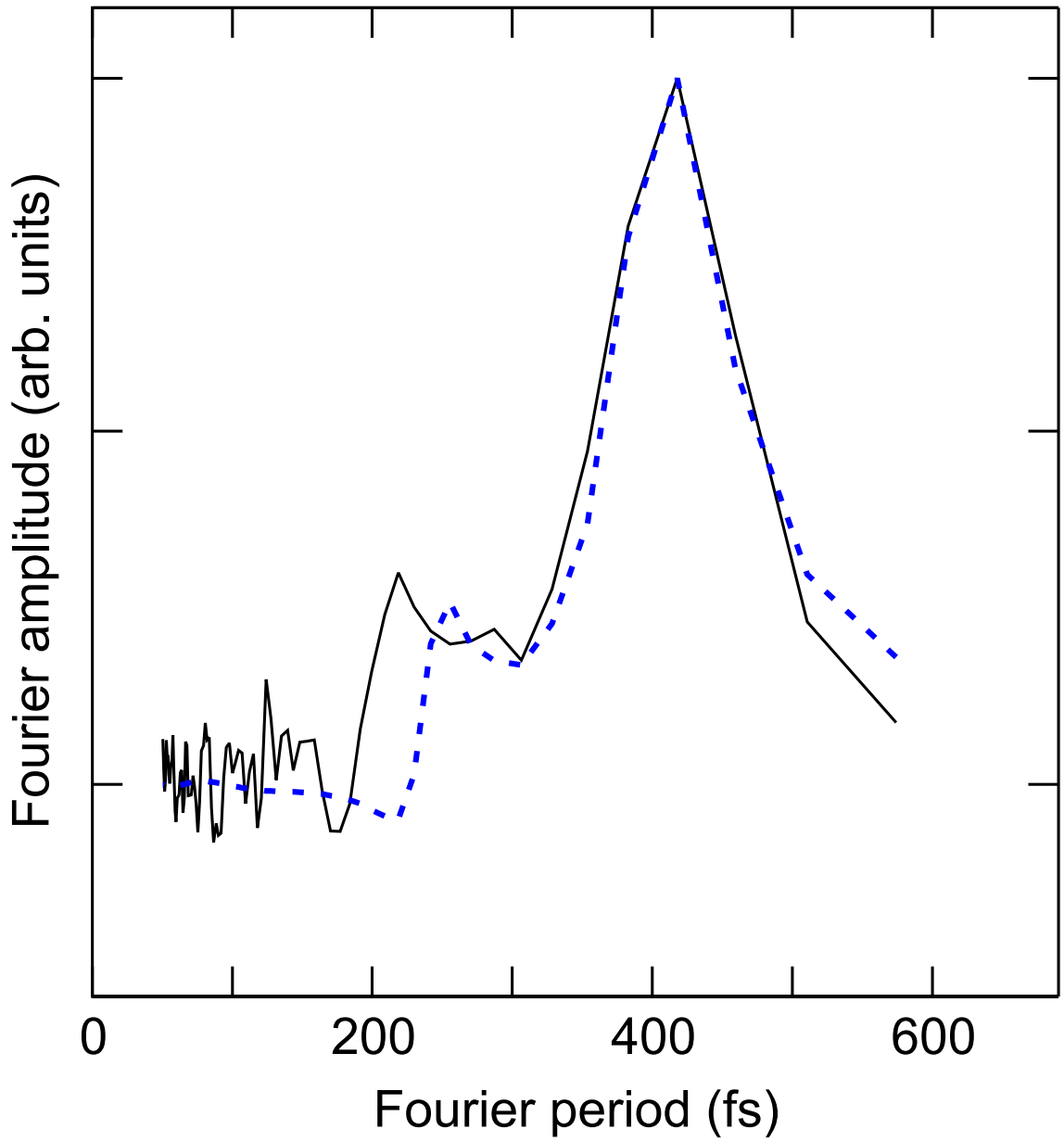


Figure 7: Fourier transform of the TDMAE$^+$ signal shown in Figure (6) for the cluster experiment (solid line) and of its simulation using Expressions (2) and (4) and the parameters listed in Table (1) (dashed line).